

# New gliding mammaliaforms from the Jurassic

Qing-Jin Meng<sup>1</sup>, David M. Grossnickle<sup>2</sup>, Di Liu<sup>1</sup>, Yu-Guang Zhang<sup>1</sup>, April I. Neander<sup>3</sup>, Qiang Ji<sup>4</sup> & Zhe-Xi Luo<sup>2,3</sup>

**Stem mammaliaforms are Mesozoic forerunners to mammals, and they offer critical evidence for the anatomical evolution and ecological diversification during the earliest mammalian history. Two new eleutherodonts from the Late Jurassic period have skin membranes and skeletal features that are adapted for gliding. Characteristics of their digits provide evidence of roosting behaviour, as in dermopterans and bats, and their feet have a calcaneal calcar to support the uropatagium as in bats. The new volant taxa are phylogenetically nested with arboreal eleutherodonts. Together, they show an evolutionary experimentation similar to the iterative evolutions of gliders within arboreal groups of marsupial and placental mammals. However, gliding eleutherodonts possess rigid interclavicle–clavicle structures, convergent to the avian furculum, and they retain shoulder girdle plesiomorphies of mammaliaforms and monotremes. Forelimb mobility required by gliding occurs at the acromion–clavicle and glenohumeral joints, is different from and convergent to the shoulder mobility at the pivotal clavicle–sternal joint in marsupial and placental gliders.**

Mammaliaforms of the Mesozoic Era (252 to 66 million years ago (Ma)) are extinct relatives of modern mammals<sup>1–3</sup>, and they provide crucial fossil evidence on diversification in the earliest mammalian history<sup>4–6</sup>. Stem mammaliaforms are morphologically disparate and ecologically diverse in their own right, and they developed versatile locomotor modes that include arboreal, semiaquatic, and subterranean specializations, which are all distinct from generalized mammaliaforms<sup>7–11</sup>. Haramiyidans are a major mammaliaform clade<sup>12–14</sup> that includes several arboreal species<sup>15,16</sup>. We further report two new volant eleutherodont haramiyidans from the Jurassic Tiaojishan Formation (approximately 160 million years old) of China. Evolution of gliding behaviour is an important evolutionary transition between divergent land-based and aerial habitats<sup>17,18</sup>. It requires considerable shoulder and forelimb manoeuvrability, which these eleutherodonts achieved in a unique way that differs from crown mammal gliders, despite a primitive shoulder girdle. Further, they are the most primitive known gliders in mammal evolution, evolving approximately 100 million years before the earliest known therian gliders. They are the first in a long history of iterative evolutions of gliders from arboreal ancestors, as occurred later in multiple extant marsupial and placental groups<sup>17–19</sup>, and in additional Mesozoic mammals<sup>20</sup>.

Clade Mammaliaformes<sup>1</sup>  
Clade Haramiyida (emended by ref. 2)  
Clade (Order) Eleutherodontida<sup>21</sup>  
*Maiopatagium furculiferum* gen. et sp. nov.

**Etymology.** *Maio* (Latin): mother; *patagium* (Latin): skin membrane, referring to the preserved patagial membranes of the fossil; *furcula* (Latin): fork; *ferum* (Latin): similar, in reference to the sutured and/or fused interclavicle and clavicles that are morphologically convergent to the furculum (wishbone) of birds.

**Holotype.** Beijing Museum of Natural History PM002940 (abbreviated hereafter as BMNH2940), with almost all bones and integumentary tissues preserved on the main shale slab (BMNH2940A) (Figs 1, 2 and Extended Data Figs 1–3; Supplementary Information Tables 1–3).

Broken fragments of incomplete, thin counter-layers of shale are still associated with the main slab. The intact main slab and the fractured counter-layer show similar ultraviolet (UV) fluorescent patterns of the preserved fur and skin membranes, interpreted as patagia consisting of propatagium, plagiopatagium and incomplete uropatagium.

## Locality and geologic age

The Daxishan fossil site of Linglongta township, Jianchang County, Liaoning Province, China. The fossil slab has preserved specimens of the index fossil *Qaidamestheria* sp. (*Euestheria luanpingensis*) that are known from the upper fossiliferous stratigraphic level of the Tiaojishan Formation<sup>22</sup>. The vertebrate-bearing level of this site is dated to be  $158.5 \pm 1.6$  to  $161.0 \pm 1.44$  million years old<sup>23</sup>. The Tiaojishan fauna has yielded several additional mammaliaforms<sup>16,24</sup>.

## Differential diagnosis

Dental formula  $I^1, P^2, M^2$ . Similar to all eleutherodonts in having a reduced post-incisor tooth count, and in having four upper premolars and molars (Fig. 2). Similar to eleutherodontids for which the skull is preserved in showing a down-turned rostrum at the long post-incisor diastema, and in having a subtemporal angle on the maxilla near the maxillary–jugal junction. Of all eleutherodonts, *M. furculiferum* is most similar to *Shenshou lui* in having a diastema between the penultimate and ultimate upper premolars, upper molars with a tight coalescence of cusps on the lingual cusp row, which becomes crest-like, and a straight and median occlusal furrow open at both ends of  $P^4$ – $M^2$ . In these features it differs from eleutherodontids<sup>16,25</sup> that lack the penultimate–ultimate premolar diastema, and show distinctive cusps on the lingual cusp row and a fusiform median occlusal basin closed at mesial and distal ends of upper molars. The lingual cusp row of *M. furculiferum* is crest-like and lacks the weak cusp division on the lingual cusp row of *S. lui*<sup>16</sup>. It has a single cusp on its upper incisor while the upper incisor is bicuspid in *S. lui*<sup>16</sup>.  $M^1$  and  $M^2$  of *Maiopatagium* are only 70% in length of the same teeth in the *Shenshou lui*<sup>16</sup>. A noteworthy skeletal feature of eleutherodonts is

<sup>1</sup>Beijing Museum of Natural History, Beijing 100050, China. <sup>2</sup>Committee on Evolutionary Biology, The University of Chicago, Chicago, Illinois 60637, USA. <sup>3</sup>Department of Organismal Biology and Anatomy, The University of Chicago, Chicago, Illinois 60637, USA. <sup>4</sup>Hebei GEO University, Shijiazhuang 050031, Hebei Province, China.

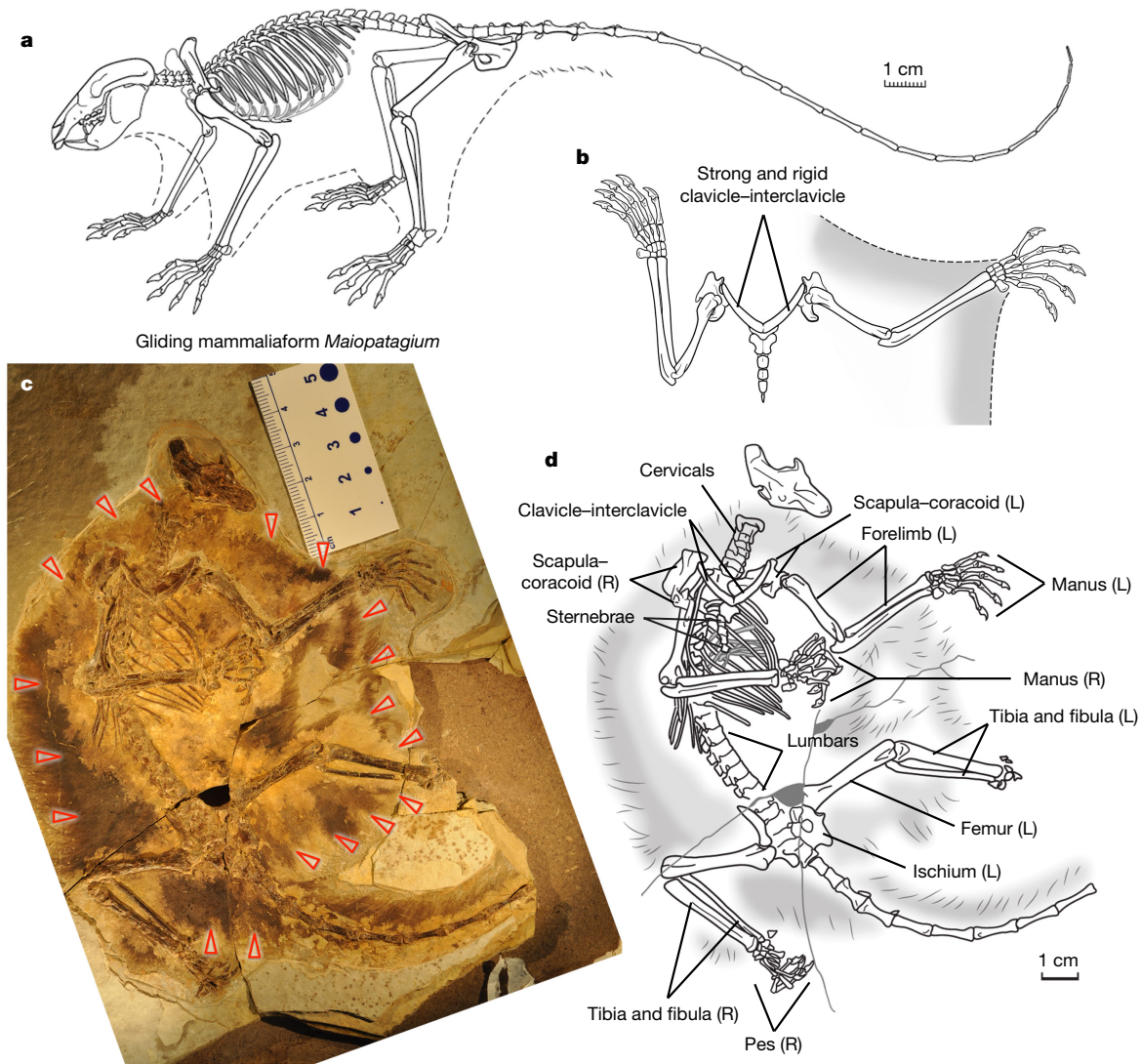


**Figure 1 | New mammaliaform *Maiopatagium furculiferum*.** **a**, Skeletal reconstruction with patagial skin membrane outlines. **b**, Shoulder girdle and forelimb reconstruction with the propatagium and plagiopatagium outlines. **c**, *M. furculiferum* holotype (BMNH2940) with patagial outlines indicated by red arrows. **d**, Structural identification. L and R indicate the

the Y-shaped clavicle–interclavicle (Fig. 3, Extended Data Figs 4–6), which is distinct from the T-shaped clavicle–interclavicles of other mammaliaforms. Extended diagnosis and taxonomic notes are provided in the Supplementary Information.

### Skin membranes and comparison to extant gliders

The pelage of *Maiopatagium* is preserved as a halo of carbonized fur of long guard hairs and short under hairs, compressed onto carbonized patagial membranes and distinct from the rock matrix under UV fluorescent light (Extended Data Fig. 1). Furthermore, we report a second eleutherodont specimen (BMNH2942) preserved with a halo of carbonized fur and patagial membranes (Extended Data Fig. 2), similar to those of *Maiopatagium*<sup>25</sup>.

Among therian mammal gliders, *Maiopatagium* (BMNH2940) and the unnamed eleutherodontid BMNH2942 (Fig. 1, Extended Data Fig. 2, see ref. 25) are most comparable to the gliding sciurid rodents owing to similar proportions of the propatagium, plagiopatagium and uropatagium<sup>19,26–28</sup>. With fully extended forelimbs and hindlimbs, the plagiopatagium is 60 mm wide from the vertebral column to the lateral edges of the membrane, extending from the wrist to the ankle (Extended Data Figs 1, 2, 7). The propatagium is about 50 mm

left and right sides of specimen, respectively. More photos of skeleton and skin membranes are provided in Extended Data Fig. 1. An additional eleutherodont with preserved skin membranes (BMNH2942)<sup>25</sup> is shown in Extended Data Fig. 2 and discussed in the Supplementary Information.

wide from the cheek of the skull to the wrist and 15 mm deep from the leading edge of the membrane to the humerus. The uropatagium extends from the pelvis and the post-pelvic caudals 3 and 4, laterally to the calcaneal calcar (described below). It is approximately 50 mm wide from the hip joint to the ankle and about 20 mm deep from the femur to the uropatagium trailing edge. The new eleutherodonts differ from gliding anomalurid rodents in which the plagiopatagium extends only to the forelimb elbow. They also differ from most rodent gliders and the marsupial greater glider (*Petauroides volans*) in lacking the styliform structure from the wrist or ulnar olecranon<sup>19,29</sup>. In addition, they differ from dermopterans in having a smaller propatagium due to shorter cervicals and a less extensive uropatagium<sup>30</sup>. Most prominently, they differ from marsupial gliders that have weakly developed propatagia and uropatagia<sup>19,28</sup>.

### Inference of locomotor modes by limb proportions

Gliding adaptations in extant mammals are correlated with the relative proportions of limb elements<sup>27,31–33</sup>. We measured and compiled data<sup>20,31,33</sup> for a large sample of modern and fossil mammals (Supplementary Information, Supplementary Tables 4–13), and performed a suite of morphometric analyses using indices (that is,



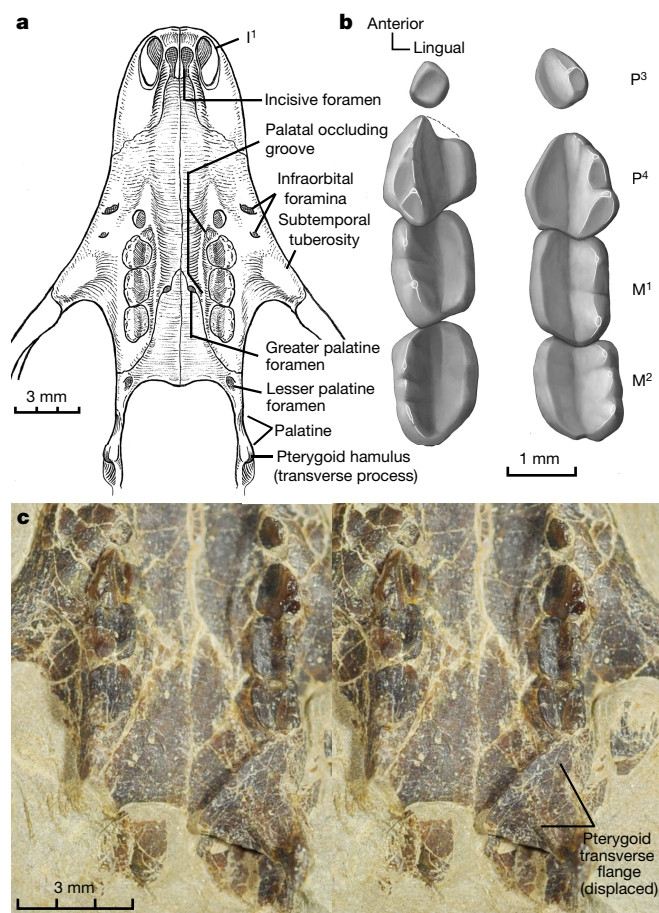


**Figure 2 | *Maiopatagium* skull.** **a**, Anterior cranium with intact upper dentition (I<sup>1</sup>, C<sup>0</sup>, P<sup>2</sup>, M<sup>2</sup>) reconstruction in ventral view. **b**, P<sup>1</sup>–M<sup>2</sup> of both sides in ventral view. Note the extensive wear on the lingual side of both tooth rows. **c**, Stereo pair photos of P<sup>1</sup>–M<sup>2</sup> of both tooth rows, and posterior palatal structure with a large transverse process of the pterygoid (homologue of the hamulus). Additional skull photos are provided in Extended Data Fig. 3.

ratios) of limb elements that are useful for differentiating gliders from non-gliding species of the same clades. For most indices, eleutherodonts overlap with the ranges for modern gliders and non-gliding arborealists, although they are closer to the mean values of modern gliders than non-gliders for several indices<sup>31–33</sup> (Fig. 4, Extended Data Figs 8 and 9), including hand proportions (Extended Data Fig. 8). However, *Shenshou* and the unnamed eleutherodont BMNH1137 are closer to the mean for non-gliding arborealists than gliders for two indices (Extended Data Fig. 9b, d), and hence they are less likely to be gliders than other eleutherodonts.

These observations for individual indices are corroborated by multivariate analyses using the results of six functional indices for 82 modern mammals<sup>31–34</sup> (Fig. 4, Extended Data Figs 8 and 9). For the linear discriminant analysis (LDA), fossils were classified as having unknown locomotor modes, and the analysis identified *Maiopatagium*, BMNH2942 and *Xianshou songae* (BMNH1137) as gliders using posterior probabilities of locomotor assignment (Fig. 4; Supplementary Table 11). For both the LDA and a principal component analysis (PCA), *Maiopatagium*, *Xianshou songae* (BMNH1137) and the eleutherodont specimens BMNH2942 and BMNH1133 occupy a similar morphospace region as extant gliders (Fig. 4, Extended Data Fig. 9). This provides strong evidence that *Maiopatagium*, BMNH2942, and *Xianshou songae* are gliders. However, *Shenshou lui* and the unnamed eleutherodont BMNH1137 are further from the PCA and LDA morphospace regions occupied by modern gliders, and the LDA does not assign them to the

gliding category (Supplementary Table 11). Thus, it is less likely that they are also gliders (Fig. 4g, f, Extended Data Fig. 9), suggesting that although all eleutherodonts are arboreal, not all are gliders.

### Shoulder girdle

Arboreal and volant adaptations require enhanced mobility at the glenohumeral and girdle joints. In gliding eleutherodonts, this is enabled by a mobile clavicle–acromion joint and an open, saddle-shaped glenoid of the scapula–coracoid (Figs 3, 4, Extended Data Figs 4–6), which is in juxtaposition to an otherwise plesiomorphic, structurally rigid sternum–clavicle–interclavicle. The two curved and gracile clavicles and a short interclavicle are sutured or fused to form a Y-shaped structure, in which the proximal 25% of the clavicle forms a rigid suture contact with the interclavicle. The two clavicles form an angle that is approximately 90° in *Maiopatagium* and 85° in BMNH2942 (Extended Data Figs 4, 5). The fused, Y-shaped clavicle–interclavicle is distinctly similar (via convergence) to avian furcula (Fig. 3, Extended Data Figs 4–6; Supplementary Video 1), but otherwise retains the plesiomorphic features of monotremes, mammaliaforms and cynodont outgroups<sup>35,36</sup>, notwithstanding minor taxonomic differences (Supplementary Information). The scapula–coracoid consists of a coracoid, a separate procoracoid perforated by a foramen, and a scapula, all of which are similar to those of non-mammalian cynodonts, *Morganucodon* and *Sinoconodon*<sup>11,35,36</sup> (Fig. 3). These separate scapula–coracoid elements can be distinguished on several specimens. In a juvenile specimen of eleutherodont BMNH3258, these elements can be virtually dissected out from an intact shoulder girdle (Figs 3, 4 and Extended Data Fig. 4). However, *Maiopatagium* and eleutherodonts are more plesiomorphic than docodonts that lack a procoracoid<sup>8</sup> and extant monotremes that have a plate-like procoracoid without a coracoid foramen, although its attachment to the rest of the girdle has shifted in position in monotremes (Figs 3, 4 and Supplementary Video 1).

The scapula–coracoid consists of a large infraspinatus muscle fossa on its entire lateral surface, with attachment of the teres major muscle at the dorsoposterior corner. As in other eleutherodonts<sup>16</sup>, the acromion is prominent and robust, and shows a round depression to receive the rounded distal end of the clavicle. This joint is synovial and mobile, allowing the scapular acromion to pivot around the distal clavicle. The glenoid at the scapula–coracoid junction is saddle-shaped and has an oval outline, allowing relatively wide dorsoventral pivotal rotation and some protraction/retraction of the humerus, despite the rigid sternum–interclavicle–clavicle structure. In this regard, *Maiopatagium* and eleutherodonts are distinct from therian mammals and multituberculates in which mobility of the shoulder girdle comes largely from the pivotal joint of the clavicle and interclavicle (or manubrium)<sup>37,38</sup>. Thus, the gliding behaviour of eleutherodonts was enabled by significant shoulder mobility at the acromion–clavicle joint and different shapes of the glenohumeral joint, in contrast to the therian gliders with increased mobility at the sternum–clavicle joint.

### Morphology and intrinsic proportions of the pes

The astragalus is an oblong bone without an astragal neck or head. The calcaneus is a wide and rectangular bone (width to length ratio of 80%) with an obtuse and short peroneal process, and a short and ventrolaterally turned calcaneal tuber. The broad width (relative to length) of the calcaneus and short calcaneal tuber are plesiomorphies shared by *Megaconus* and *Morganucodon*<sup>14</sup>. The rectangular outline and the short tuber of the calcaneus are similar to monotremes<sup>14,39</sup>. *Maiopatagium* and BMNH1133 both show a cone-shaped calcar that articulates via a V-shaped joint with the calcaneal tuber (Fig. 4, Extended Data Fig. 7). The calcar bears a resemblance to the short calcar of some phyllostomid bats, although the calcar has a wider range of morphologies in other bats. It is also noteworthy that the eleutherodont calcar is wider at the base than the calcar in bats<sup>40,41</sup>. In BMNH1133 and *Shenshou* (personal observation), the calcar is distinguishable from the os calcis for the extratarsal spur. The calcar

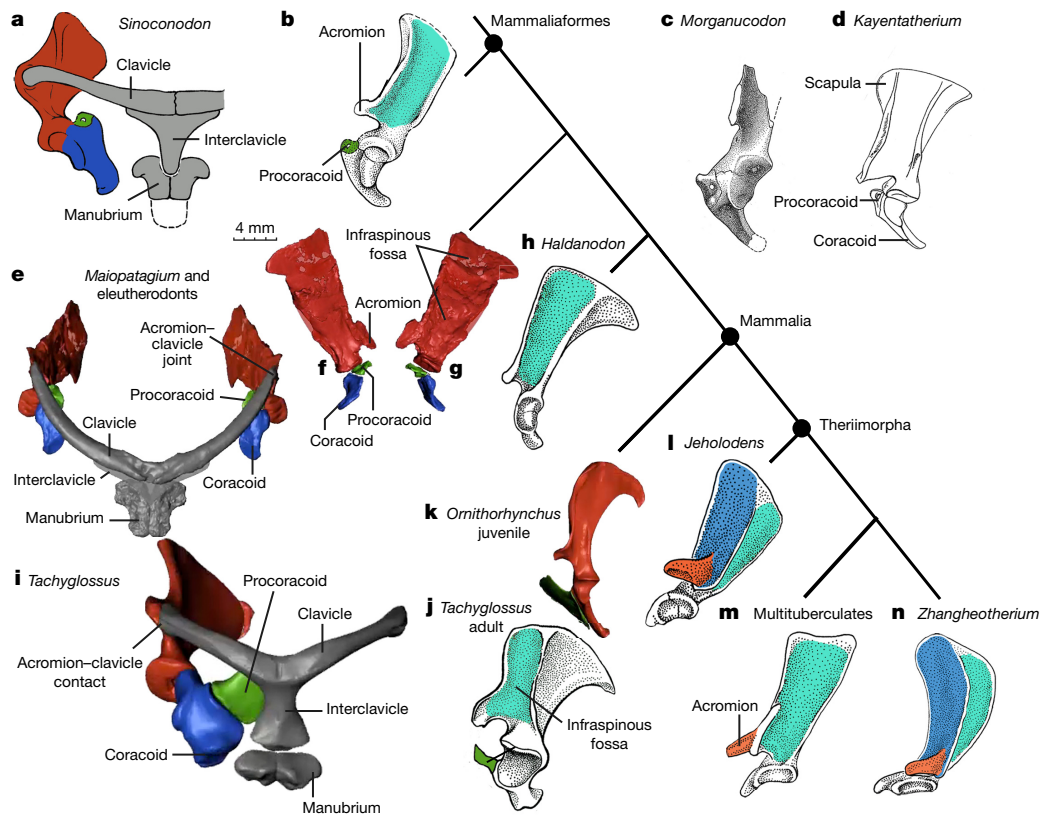


**Figure 3 | Evolution of shoulder girdle among mammaliaforms.**

**a, b**, *Sinoconodon* shoulder girdle in ventral view (**a**) and scapulocoracoid in lateral view (**b**). **c**, *Morganucodon* (from ref. 11). **d**, *Kayentatherium* (from ref. 35). **e–g**, Eleutherodont shoulder girdle in ventral view (**e**), and the scapula–coracoid in medial (**f**) and lateral (**g**) views (from computed tomography scans of BMNH3258). See Supplementary Video 1 and Extended Data Figs 4 and 5 for further details

from additional eleutherodonts. **h**, Docodont *Haldanodon* (from ref. 8). **i–k**, Monotremes: shoulder girdle (details in Supplementary Video 1), and the procoracoid, coracoid and scapula of an adult *Tachyglossus* (**j**) and a juvenile *Ornithorhynchus* (**k**), both in lateral view. **l**, Eutriconodont *Jeholodens* (from ref. 36). **m**, Generalized multituberculate. **n**, Spalacotherioid *Zhangheotherium* (from ref. 35).

coexists with the os calcareus preserved near the distal tibia and fibula (Extended Data Fig. 7).

Each proximal pedal phalanx has a pronounced longitudinal groove on its flexor aspect for the flexor digitorum profundus tendon. This groove is usually well developed in mammals with enhanced grasping capabilities, such as arboreal didelphids, arboreal rodents, and in Cretaceous mammals inferred to be scansorial or arboreal<sup>42,43</sup>. The flexor digitorum profundus is especially well developed in the proximal pedal phalanges of volant bats and dermopterans that are capable of roosting posture by habitually flexing their pedal digits to grab suspending structures, enhanced by tendon-locking mechanism associated with the well-developed flexor digitorum profundus<sup>44</sup>. At minimum, this structure suggests that the flexor digitorum profundus is well-developed and deeply pressed into its tendon groove on the phalanges, as in extant mammals with an enhanced capacity for grasping.

Eleutherodonts have elongated proximal and intermediate phalanges, relative to the short metatarsals<sup>15,16</sup> (Fig. 4). The pedal phalangeal index ((proximal + intermediate phalangeal lengths)/metatarsal length) values of eleutherodonts (including *Maiopatagium*) are greater than those of arboreal dermopterans and primates, and are comparable to or surpass those of bats (Fig. 4).

Bats have five pedal digits of subequal length to grip suspending structures for roosting<sup>44</sup>. By comparison, digit ray 1 of eleutherodonts is shorter than digit rays 2–5, plesiomorphically as in typical mammals, and different from pedal digit 1 of bats. Nonetheless, the elongated digit rays 2–5 at subequal lengths show strong resemblance to the pedal

digits of equal length in bats that are specialized for grasping during roosting (Fig. 4).

### Morphology and intrinsic proportions of the manus

The manual digit rays of eleutherodonts have greatly elongated proximal and intermediate phalanges. The hand digital segment proportions are very similar to those of pedes<sup>16</sup>. Notably, the manual phalangeal index of eleutherodonts far surpasses those of arboreal mammals<sup>33</sup>, and is comparable to the pedal phalangeal proportions of bats specialized for pedal roosting (Fig. 4). The manus digit rays 2–5 of eleutherodontids are also subequal, very similar to the manual digit rays 2–5 of dermopterans that also use their hands for upside-down suspension in four-limb roosting<sup>45</sup>. Thus, based on the hand and foot characteristics, we hypothesize that eleutherodonts have similar roosting behaviour to extant volant dermopterans, although the pedal and manual characteristics match more closely with chiropteran pedal structures (Fig. 1).

### Inference on molar function and diet

Extant mammalian gliders are all herbivores (or plant-dominated omnivores) and their main dietary categories are granivory, folivory, frugivory and exudativory, although these diets are supplemented with insects and other miscellaneous sources<sup>19,46</sup>. The intact upper tooth rows of *Maiopatagium* have bi-serial cusp rows or ridges on the molars, most similar to those of megachiropteran bats<sup>47</sup> (for example, *Hypsignathus* in Extended Data Fig. 3). To some extent, the teeth of *Maiopatagium* are also similar to the lingual grinding surface on the molars of some phyllostomid bats that evolved secondary



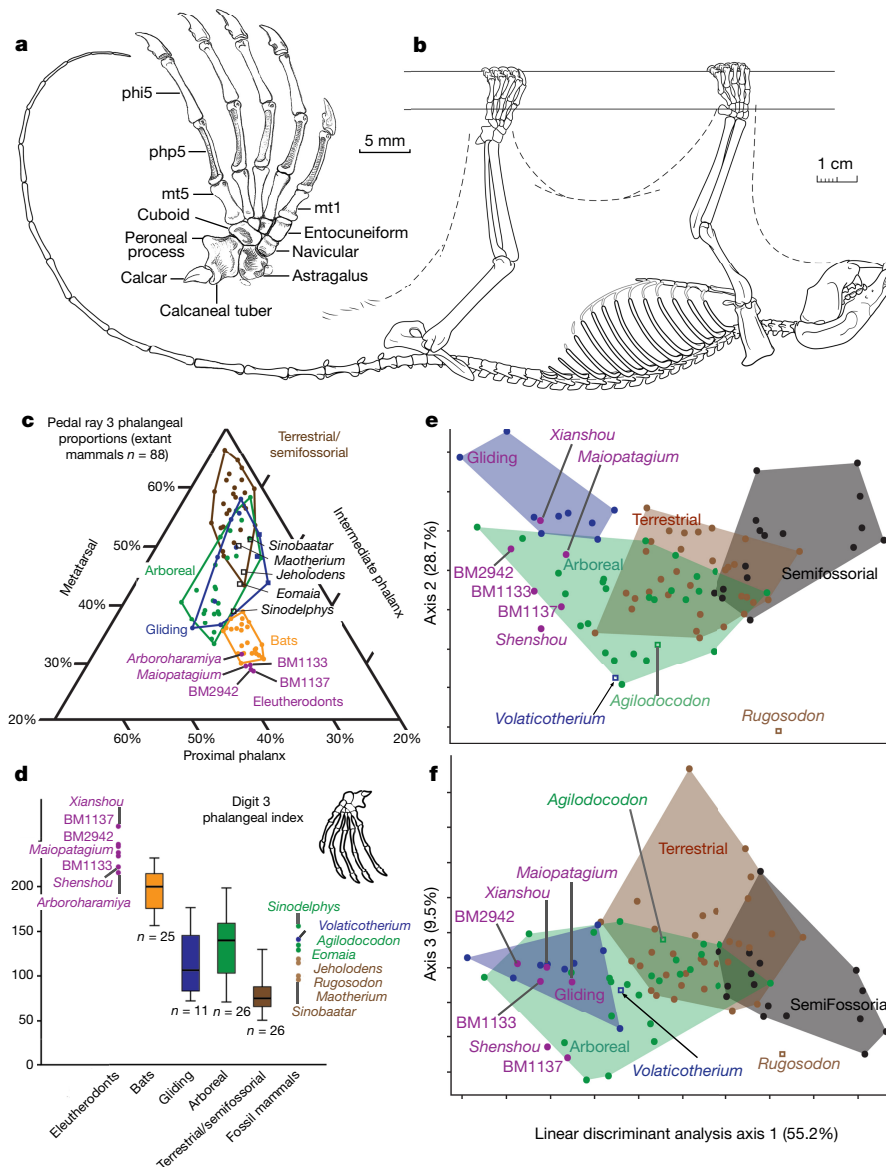


**Figure 4 | Foot structure of eleutherodonts for gliding and roosting behaviours, and limb skeletal morphometrics for inference of locomotor modes and substrate preferences.** **a**, Pes reconstruction, based on BMNH2940 and BMNH1133 (see Extended Data Fig. 7). The calcar is in articulation with the calcaneal tuber and the proximal phalanges show the flexor groove. mt, metatarsal; phi, phalanx-intermediate; php, phalanx-proximal. **b**, Reconstruction of the *Maiopatagium* skeleton with skin membranes in roosting posture. **c**, Ternary diagram of pedal digit 3 proportions of eleutherodonts and extant mammal ecomorphotypes. In pedal metatarsal–phalangeal proportions, eleutherodonts are most similar to extant bats. This suggests that eleutherodonts and bats are similar in pedal function and substrate contact, and the former probably relied on pedal digit grasping as seen in the roosting behaviour of bats. **d**, Pedal 3 phalangeal index ((proximal + intermediate phalangeal lengths)/metatarsal length  $\times 100$ ). Eleutherodonts are most similar to volant chiropterans. Upper and lower box boundaries represent 25% and 75% quartiles, and whisker lines represent the range. **e**, **f**, Multivariate LDA of extant mammal ecomorphotypes, including gliders. Fossil taxa are treated as ‘unknowns’ and not assigned to a locomotor mode. *Maiopatagium* is nested most closely to extant gliders in both the axes 1 and 2 of the plot in **e** and axes 1 and 3 of the plot in **f**. *Xianshou songae* and two other eleutherodonts (BMNH2942 and BMNH1133) are also closely associated with the glider morphospace region. Eleutherodontid BMNH1137 and *Shenshou* are more closely associated with extant arboreal taxa, especially along axes 2 and 3. Additional analyses are presented in Extended Data Figs 8 and 9.

specialization for frugivory<sup>48</sup>. From these dental similarities, we infer that *Maiopatagium* was analogous to herbivorous bats, having a primarily herbivorous diet of ferns and gymnosperm plants that are known from the Late Jurassic. We speculate that Jurassic eleutherodonts fed on soft plant parts, such as young leaves, tender meristem tissues, exposed tissues of stroboli and cones, and possibly the tender tissues of the recessed ovulates of seed ferns and various gymnosperm plants that were common for animal herbivory<sup>49</sup>. Because angiosperms had yet to evolve in the Late Jurassic<sup>49</sup>, the feeding by *Maiopatagium* on soft plant tissues is functionally analogous to the frugivory of Cenozoic herbivorous bats on angiosperm fruits<sup>47,48</sup>.

**Evolutionary implications**  
Although not as abundant as dinosaurs during Mesozoic, early mammals nonetheless developed many of the divergent ecomorphotypes that later became common in crown mammals<sup>4–6,32</sup>. Mesozoic mammal clades also evolved some degree of within-group ecological diversification, as evidenced by eutriconodonts, spalacotherioids, multituberculates and crown therians<sup>6,32,49,50</sup>. Even before the rise of crown mammals, stem mammaliaform groups also showed significant palaeoecological diversity, most notably by docodonts<sup>7–9,13</sup>. The new gliding forms among eleutherodonts suggest that this clade, too, exploited new niches otherwise inaccessible for additional

mammaliaforms and vertebrates. The inferred volant locomotion of these gliders is consistent with their dental morphology that suggests a primarily herbivorous diet. This is a recurrent pattern in the evolution of herbivorous (or plant-dominated omnivorous) gliders among therians. The volant *Maiopatagium* and other eleutherodonts are phylogenetically nested within the eleutherodont clade of mainly arboreal species. As stem mammaliaforms, these fossils provide the earliest known case of an iterative and widespread pattern in which volant mammals derived from arboreal ancestors, took to the air, and transitioned between very divergent habitats.

**Online Content** Methods, along with any additional Extended Data display items and Source Data, are available in the online version of the paper; references unique to these sections appear only in the online paper.

**Data Availability** Specimens of this study are accessioned in Beijing Museum of Natural History (BMNH2940, BMNH2942, BMNH3253, BMNH3528). Graphics and phylogenetics data for this study are provided in the Supplementary Information. Life Science Identifier (LSID) (<http://zoobank.org/registration>): urn:lsid:zoobank.org:act: urn:lsid:zoobank.org:pub:68A81281-1BA0-4B7B-9B25-F067F5FF47B.

Received 23 October 2016; accepted 12 July 2017.

Published online 9 August 2017.

- Rowe, T. B. Definition, diagnosis, and origin of Mammalia. *J. Vertebr. Paleontol.* **8**, 241–264 (1988).
- Kielan-Jaworowska, Z., Cifelli, R. L. & Luo, Z.-X. *Mammals from the Age of Dinosaurs: Origins, Evolution, and Structure* (Columbia Univ. Press, New York, 2004).
- Kemp, T. S. *The Origin and Evolution of Mammals* (Oxford Univ. Press, Oxford, 2005).
- Luo, Z.-X. Transformation and diversification in early mammal evolution. *Nature* **450**, 1011–1019 (2007).
- Close, R. A., Friedman, M., Lloyd, G. T. & Benson, R. B. Evidence for a mid-Jurassic adaptive radiation in mammals. *Curr. Biol.* **25**, 2137–2142 (2015).
- Grossnickle, D. M. & Polly, P. D. Mammal disparity decreases during the Cretaceous angiosperm radiation. *Proc. R. Soc. Lond. B* **280**, 20132110 (2013).
- Ji, Q., Luo, Z. X., Yuan, C. X. & Tabrum, A. R. A swimming mammaliaform from the Middle Jurassic and ecomorphological diversification of early mammals. *Science* **311**, 1123–1127 (2006).
- Martin, T. Postcranial anatomy of *Haldanodon expectatus* (Mammalia, Docodontia) from the Late Jurassic (Kimmeridgian) of Portugal and its bearing for mammalian evolution. *Zool. J. Linn. Soc.* **145**, 219–248 (2005).
- Meng, Q.-J. *et al.* An arboreal docodont from the Jurassic and mammaliaform ecological diversification. *Science* **347**, 764–768 (2015).
- Luo, Z.-X., Gatesy, S. M., Jenkins, F. A. Jr, Amaral, W. W. & Shubin, N. H. Mandibular and dental characteristics of Late Triassic mammaliaform *Haramiyavia* and their ramifications for basal mammal evolution. *Proc. Natl Acad. Sci. USA* **112**, E7101–E7109 (2015).
- Jenkins, F. A. Jr & Parrington, F. R. The postcranial skeletons of the Triassic mammals *Eozostrodon*, *Megazostrodon* and *Erythrotherium*. *Phil. Trans. Royal Soc. B* **273**, 387–431 (1976).
- Jenkins, F. A. Jr, Gatesy, S. M., Shubin, N. H. & Amaral, W. W. Haramiyids and Triassic mammalian evolution. *Nature* **385**, 715–718 (1997).
- Luo, Z.-X. *et al.* Evolutionary development in basal mammaliaforms as revealed by a docodontan. *Science* **347**, 760–764 (2015).
- Zhou, C.-F., Wu, S., Martin, T. & Luo, Z. X. A Jurassic mammaliaform and the earliest mammalian evolutionary adaptations. *Nature* **500**, 163–167 (2013).
- Zheng, X., Bi, S., Wang, X. & Meng, J. A new arboreal haramiyid shows the diversity of crown mammals in the Jurassic period. *Nature* **500**, 199–202 (2013).
- Bi, S., Wang, Y., Guan, J., Sheng, X. & Meng, J. Three new Jurassic euharamiyidan species reinforce early divergence of mammals. *Nature* **514**, 579–584 (2014).
- Dudley, R. *et al.* Gliding and the functional origins of flight: biomechanical novelty or necessity? *Annu. Rev. Ecol. Syst.* **38**, 179–201 (2007).
- Socha, J. J. *et al.* How animals glide: from trajectory to morphology. *Can. J. Zool.* **93**, 901–924 (2015).
- Jackson, S. M. *Gliding Mammals of the World* (CSIRO Publishing, Collingwood, Victoria, 2012).
- Meng, J., Hu, Y., Wang, Y., Wang, X. & Li, C. A Mesozoic gliding mammal from northeastern China. *Nature* **444**, 889–893 (2006).
- Kermack, K. A. *et al.* New multituberculate-like teeth from the Middle Jurassic of England. *Acta Palaeontol. Pol.* **43**, 581–606 (1998).
- Huang, D.-Y. Yanliao Biota and Yanshan Movement. *Acta Palaeontologica Sin.* **54**, 501–546 (2015).
- Liu, Y.-Q. *et al.* Timing of the earliest known feathered dinosaurs and transitional pterosaurs older than the Jehol Biota. *Palaeogeogr. Palaeoclimatol. Palaeoecol.* **323–325**, 1–12 (2012).
- Yuan, C. X., Ji, Q., Meng, Q. J., Tabrum, A. R. & Luo, Z. X. Earliest evolution of multituberculate mammals revealed by a new Jurassic fossil. *Science* **341**, 779–783 (2013).
- Luo, Z.-X. *et al.* New evidence for mammaliaform ear evolution and feeding adaptation in a Jurassic ecosystem. *Nature* <http://dx.doi.org/10.1038/nature23483> (2017).
- Thorington, R. W. Jr & Heaney, L. R. Body proportions and gliding adaptations of flying squirrels (Petauristinae). *J. Mamm.* **62**, 101–114 (1981).
- Thorington, R. W. Jr & Santana, E. M. How to make a flying squirrel: *Glaucomys* anatomy in phylogenetic perspective. *J. Mamm.* **88**, 882–896 (2007).
- Johnson-Murray, J. L. The comparative myology of the gliding membranes of *Acrobates*, *Peauroides* and *Petaurus* contrasted with the cutaneous myology of *Hemibelideus* and *Pseudochirus* (Marsupialia, Phalangeridae) and with selected gliding Rodentia (Sciuridae and Anomaluridae). *Aust. J. Zool.* **35**, 101–113 (1987).
- Thorington, R. W. Jr & Stafford, B. J. Homologies of the carpal bones in flying squirrels (Pteromyiinae): A review. *Mammal Study* **26**, 61–68 (2001).
- Kawashima, T., Murakami, K., Takayanagi, M. & Sato, F. Evolutionary transformation of the cervicobrachial plexus in the colugo (Cynocephalidae: Dermoptera) with a comparison to treeshrews (Tupaiaidae: Scandentia) and strepsirrhines (Strepsirrhini: Primates). *Folia Morphol. (Warsz)* **71**, 228–239 (2012).
- Samuels, J. X. & Van Valkenburgh, B. Skeletal indicators of locomotor adaptations in living and extinct rodents. *J. Morphol.* **269**, 1387–1411 (2008).
- Chen, M. & Wilson, G. P. A multivariate approach to infer locomotor modes in Mesozoic mammals. *Paleobiology* **41**, 280–312 (2015).
- Kirk, E. C., Lemelin, P., Hamrick, M. W., Boyer, D. M. & Bloch, J. I. Intrinsic hand proportions of euarchontans and other mammals: implications for the locomotor behavior of plesiadapiforms. *J. Hum. Evol.* **55**, 278–299 (2008).
- Hammer, Ø., Harper, D. A. T. & Ryan, P. D. PAST—PALaeontological Statistics, version 1.89. *University of Oslo, Oslo* 1–31 (2009).
- Sues, H.-D. & Jenkins, F. A. Jr in *Amniote Paleobiology: Perspectives on the Evolution of Mammals, Birds, and Reptiles* (eds M. T. Carrano *et al.*) 114–152 (Univ. Chicago Press, Chicago, 2006).
- Luo, Z.-X. in *Great Transformations: Major Events in the History of Vertebrate Life* (eds K. P. Dial *et al.*) 167–187 (Univ. Chicago Press, Chicago, 2015).
- Jenkins, F. A. Jr & Weijers, W. A. The functional anatomy of the shoulder in the Virginia opossum (*Didelphis virginiana*). *J. Zool.* **188**, 379–410 (1979).
- Sereno, P. C. in *Amniote Paleobiology: Perspectives on the Evolution of Mammals, Birds, and Reptiles* (eds M. T. Carrano *et al.*) 315–366 (Univ. Chicago Press, Chicago, 2006).
- Szalay, F. S. *Evolutionary History of the Marsupials and an Analysis of Osteological Characters* (Cambridge Univ. Press, Cambridge, 1994).
- Schutt, W. A. Jr & Simmons, N. B. Morphology and homology of the chiropteran calcar, with comments on the phylogenetic relationships of *Archaeopteropus*. *J. Mamm. Evol.* **5**, 1–32 (1998).
- Stanchak, K. E. & Santana, S. E. The calcar: a novel hind limb structure in bats. *Anat. Rec.* **299**, 244 (2016).
- Argot, C. Functional-adaptive anatomy of the forelimb in the Didelphidae, and the paleobiology of the Paleocene marsupials *Mayulestes ferox* and *Pucadelphys andinus*. *J. Morphol.* **247**, 51–79 (2001).
- Luo, Z.-X., Ji, Q., Wible, J. R. & Yuan, C. X. An Early Cretaceous tribosphenic mammal and metatherian evolution. *Science* **302**, 1934–1940 (2003).
- Simmons, N. B. & Quinn, T. H. Evolution of the digital tendon locking mechanism in bats and dermopterans: a phylogenetic perspective. *J. Mamm. Evol.* **2**, 231–254 (1994).
- Lessertisseur, J. & Saban, R. in *Traité de Zoologie Tome XVI Mammifères: Teguments et Skelettes Fascicle I* (ed. Grassé, P.-P.) 709–1078 (Masson, Paris, 1967).
- Byrnes, G. & Spence, A. J. Ecological and biomechanical insights into the evolution of gliding in mammals. *Integr. Comp. Biol.* **51**, 991–1001 (2011).
- Giannini, N. P., Wible, J. R. & Simmons, N. B. On the cranial osteology of Chiroptera. I. *Pteropus* (Megachiroptera: Pteropodidae). *Bull. Am. Mus. Nat. Hist.* **295**, 1–134 (2006).
- Santana, S. E., Strait, S. & Dumont, E. R. The better to eat you with: functional correlates of tooth structure in bats. *Funct. Ecol.* **25**, 839–847 (2011).
- Labandeira, C. C. The pollination of Mid Mesozoic seed plants and the early history of long-proboscid insects. *Ann. Mo. Bot. Gard.* **97**, 469–513 (2010).
- Wilson, G. P. *et al.* Adaptive radiation of multituberculate mammals before the extinction of dinosaurs. *Nature* **483**, 457–460 (2012).

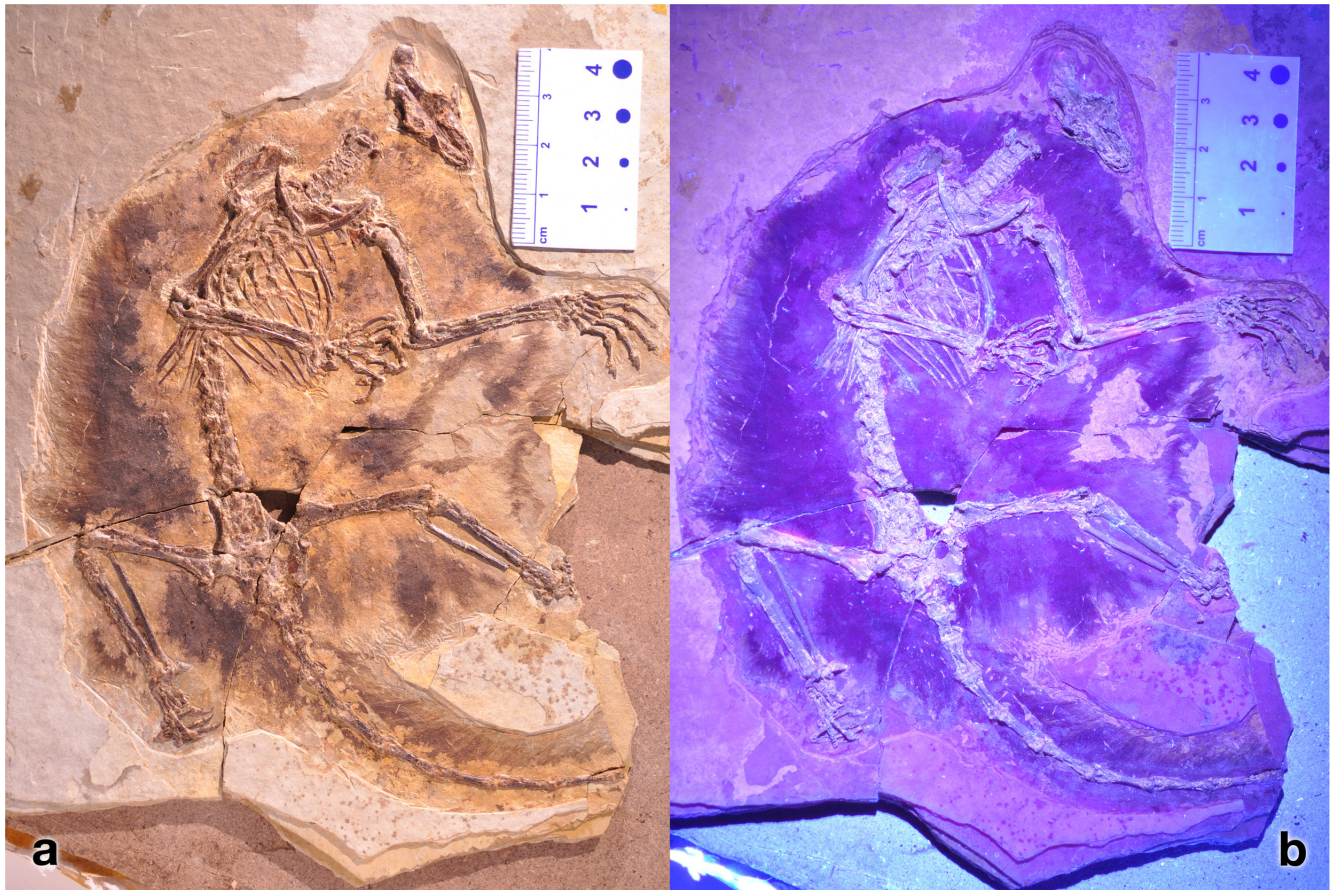
**Supplementary Information** is available in the online version of the paper.

**Acknowledgements** We thank A. Shinya for fossil preparation; S. Bi, S. Gatesy, L. Heaney, H.-J. Li, Z.-J. Gao, T. Martin, B. Patterson, P. Sereno, N. Shubin, X.-T. Zheng and C.-F. Zhou for access to comparative specimens; staff of BMNH and FMNH for assistance. Research supported by funding for Q.-J.M. (Beijing Scientific Commission), Z.-X.L. (UChicago-BSD) and D.M.G. (UChicago and FMNH Fellowships). Full acknowledgments are provided in the Supplementary Information.

**Author Contributions** Q.-J.M. and Z.-X.L. conceived the project; Q.-J.M., Y.-G.Z., D.L. and Q.J. acquired fossils and studied stratigraphy; all authors were involved in fossil interpretation during lab preparation; D.M.G. performed morphometric analyses; A.I.N. scanned and segmented fossils, prepared graphics; Z.-X.L. composed figures; Z.-X.L., Q.-J.M. and D.M.G. led the writing, with feedback from all authors.

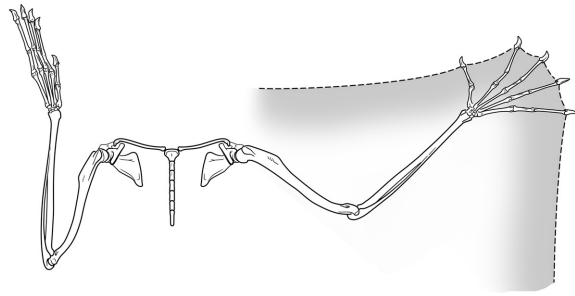
**Author Information** Reprints and permissions information is available at [www.nature.com/reprints](http://www.nature.com/reprints). The authors declare no competing financial interests. Readers are welcome to comment on the online version of the paper. Publisher's note: Springer Nature remains neutral with regard to jurisdictional claims in published maps and institutional affiliations. Correspondence and requests for materials should be addressed to Z.-X.L. ([zxluo@uchicago.edu](mailto:zxluo@uchicago.edu)).



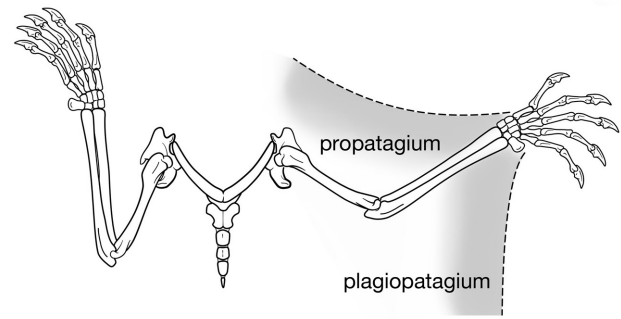


**Extended Data Figure 1 | Skin membranes of *Maiopatagium furculiferum* (holotype specimen BMNH2940).** **a**, Photograph under regular light. **b**, Photograph under UV light that enhances the fossilized soft tissue structures such as skin membranes and fur.

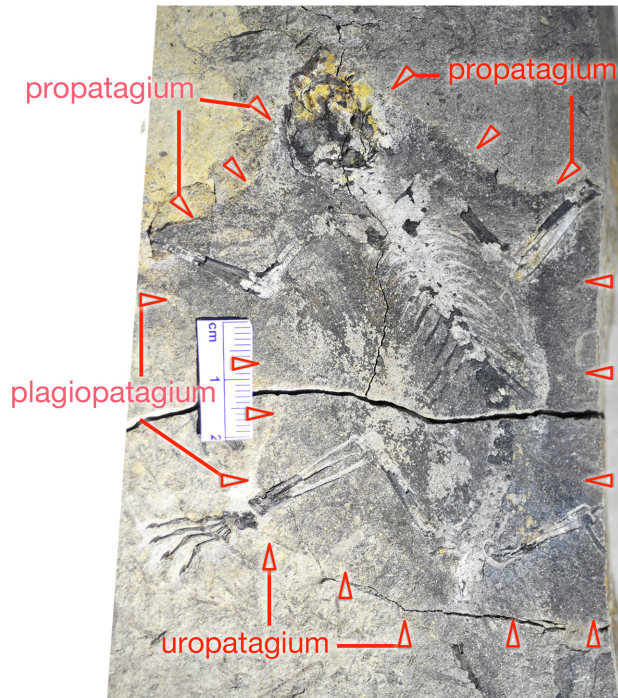




**a. *Cynocephalus*: shoulder, forelimb and skin membranes**



**b. *Maiopatagium*: shoulder, forelimb and skin membrane reconstruction**



**c. Patagial membranes preserved with BM2942B**

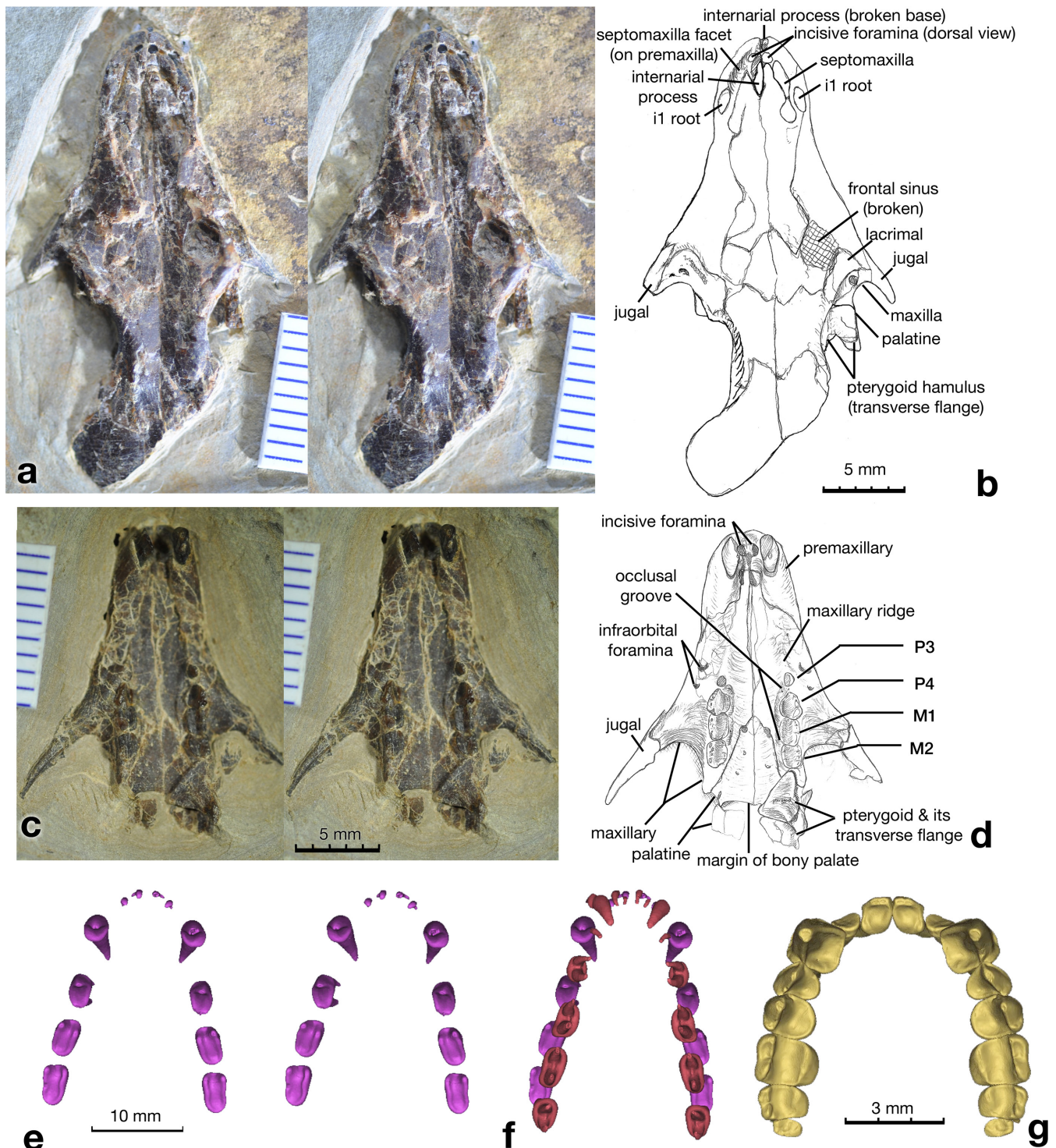


**d. Patagial membranes preserved with BM2942A**

**Extended Data Figure 2 | Fossilized skin membranes of gliding eleutherodonts and comparative morphology with extant dermopteran mammals.** **a**, Extant dermopteran *Cynocephalus*: anatomical relationship of the propatagium, the manual digital webbing, and the plagiopatagium to the forelimb and hand. **b**, Gliding eleutherodonts: relationship of the propatagium and plagiopatagium to the forelimb and manus, based on *in situ* preservation of the membranes with intact forelimbs of

*Maiopatagium furculiferum* (BMNH2940) and BMNH2942. **c**, **d**, Eleutherodont BMNH2942 with matching outlines of the propatagium, plagiopatagium and uropatagium on both slabs, BMNH2942B (**c**) and BMNH2942A (**d**). Red arrows indicate the margins of propatagium, plagiopatagium and uropatagium for BMNH2942B and the propatagium and plagiopatagium for BMNH2942A.

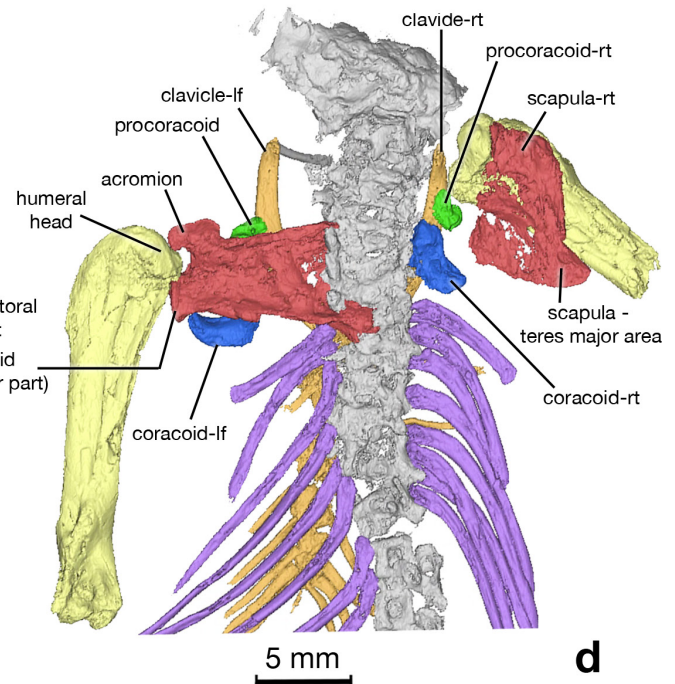
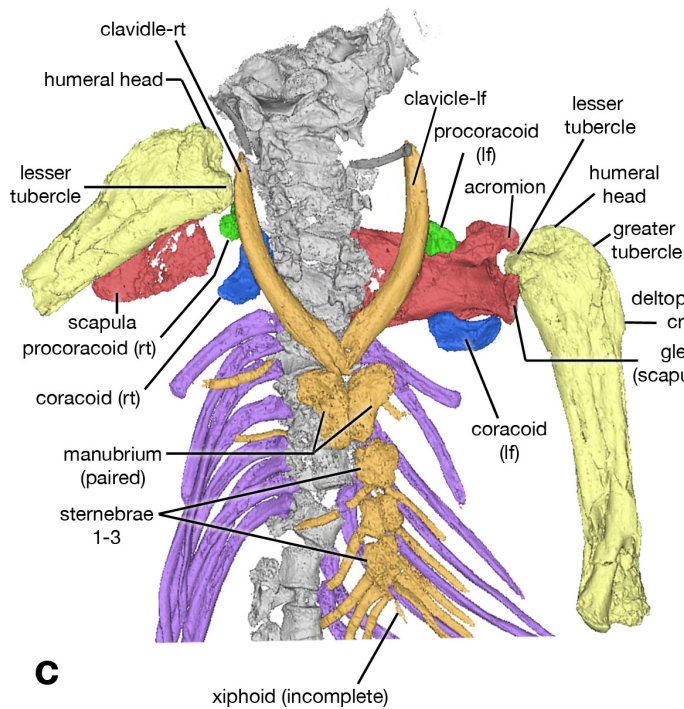
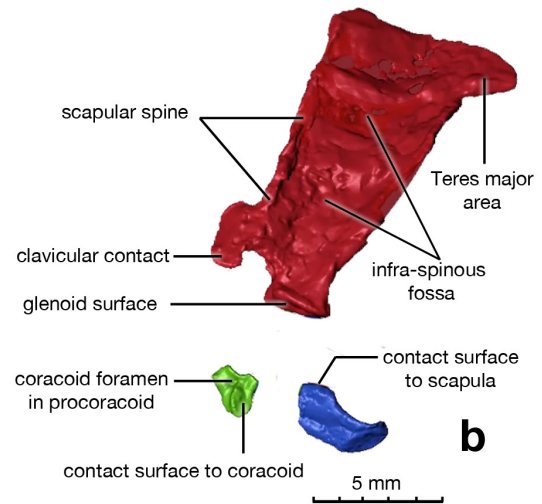
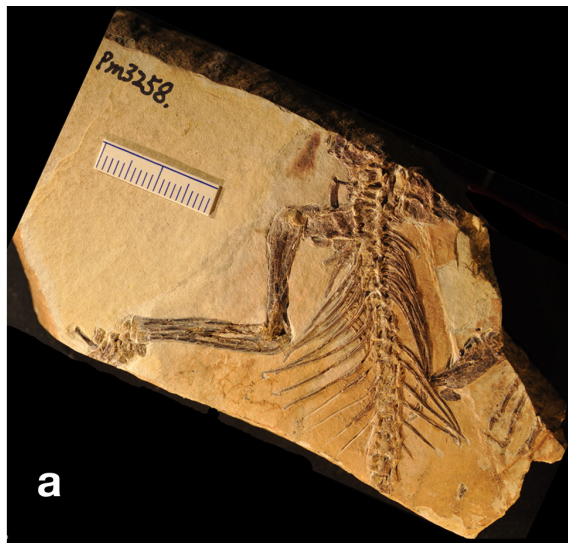




**Extended Data Figure 3 | Skull and teeth of *Maiopatagium furculiferum* (holotype BMNH2940).** **a, b**, Stereo pair photographs (**a**) and camera lucida drawing (**b**) of the dorsal view of the preserved skull. **c, d**, Stereo pair photos (**c**) and camera lucida outlines for structural identification (**d**) of the anterior part of the skull of *Maiopatagium* (BMNH2940) in ventral view as prepared from the underside of the fossil slab. **e**, Stereo pair images obtained by computed tomography (CT) scanning of the upper dentition of the megachiropteran fruit bat *Hypsignathus* in occlusal view (University of Chicago teaching collection). The bi-serial cusp rows

of upper molars are functionally analogous to the upper premolars and molars of *Maiopatagium*. **f**, Occlusal view of *Hypsignathus* upper (purple) and lower (red) tooth rows. Note that lower molars are lingual (internal) to the upper molars (purple). **g**, Phyllostomid bat *Sturnira lilium* (FMNH105870): upper premolars and molars with taller labial cusp row and lower lingual platform specialized for a frugivorous diet<sup>48</sup>. We consider phyllostomid megachiropteran *Hypsignathus* and phyllostomid *Sturnira* to be dietary analogues to *Maiopatagium* and possibly to *Shenshou*.

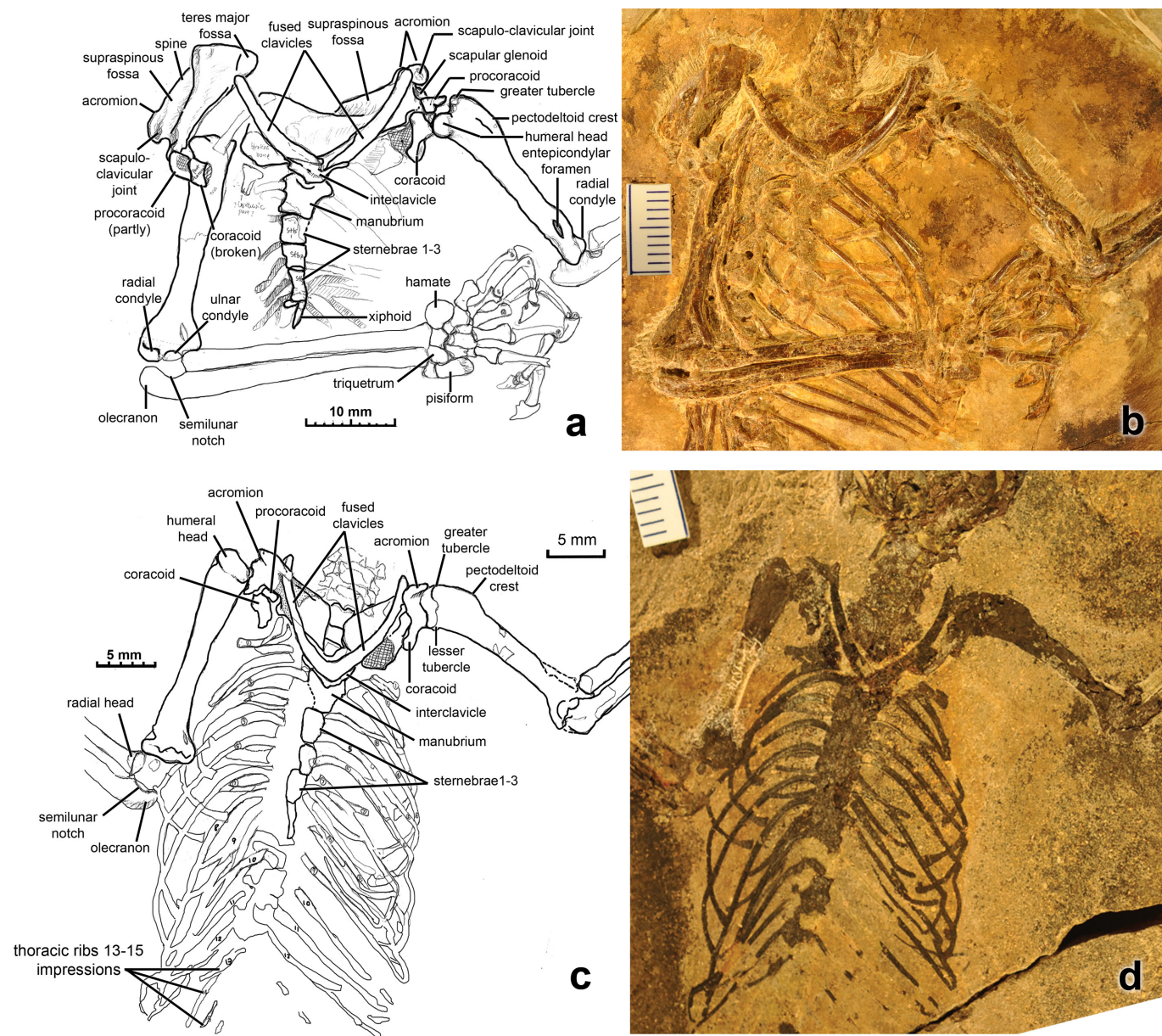




**Extended Data Figure 4 | Shoulder girdle structures of an eleutherodont (BMNH3258).** **a.** Juvenile specimen that has the lower permanent premolar half-erupted to replace the deciduous premolar that is only represented by root alveoli at the ultimate premolar locus;  $M_1$  crown present but the roots not yet formed. **b.** CT scan images of the scapula-coracoid complex in ventral view, virtually disarticulated to show structural details. The scapular plate (red) is a composite from complementary parts preserved on the left and right scapulae. The procoracoid (green) shows the coracoid foramen and a well defined

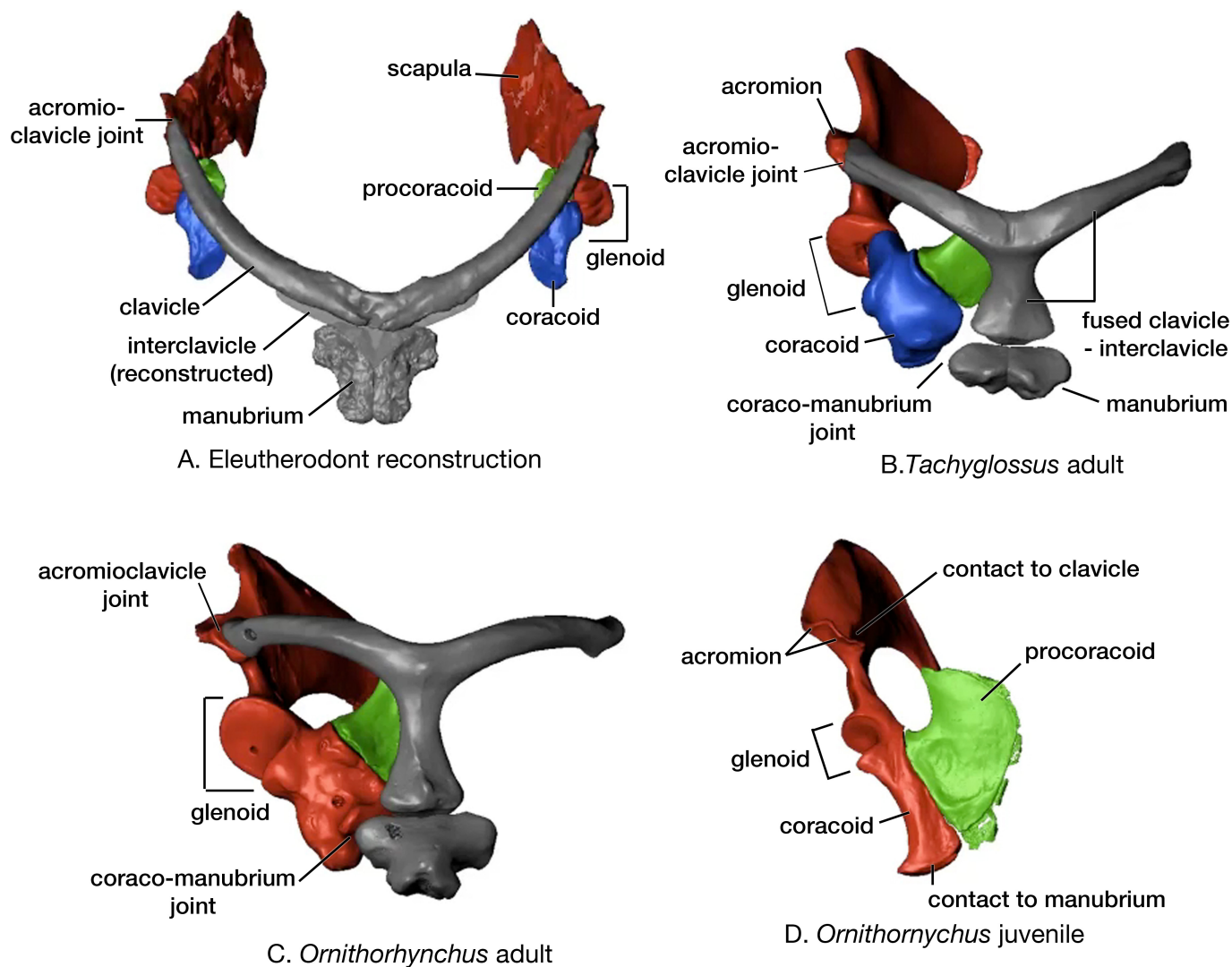
contact surface for the coracoid (blue). **c.** Shoulder girdle structures imaged from CT scans in ventral view. **d.** Shoulder girdle structures in dorsal view. Bones are coloured as follows: humerus, yellow; scapula, red; procoracoid, green; coracoid, blue; clavicles, brown; sternal series of paired manubrium, sternbrae 1-3, and a gracile xiphoid are coloured brown; the partially rendered costal ribs, brown; thoracic (dorsal) ribs, purple; vertebral column, grey. Because this is a young specimen, the interclavicle is not fully ossified. Supplementary Video 1 shows the full extent of BMNH3258 imaged by CT scans.





**Extended Data Figure 5 | Shoulder girdle and forelimb structures of eleutherodonts. a, b, *Maiopatagium furculiferum* (holotype, BMNH2940):** details of shoulder girdle and forelimbs as preserved. **c, d, A new, unnamed eleutherodont BMNH2942 (see also ref. 25):** preserved structures of

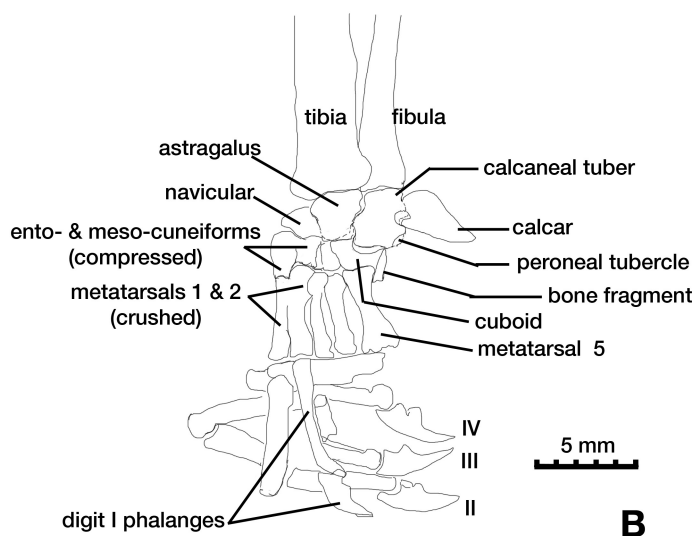
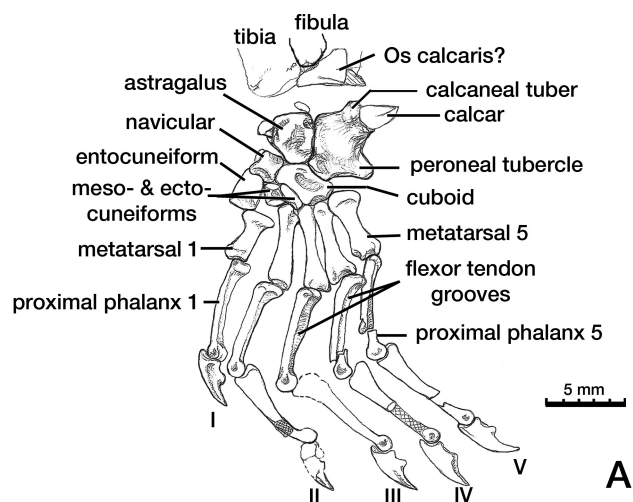
shoulder girdle on the main slab (BMNH2942A). The interclavicle is fully ossified in BMNH2940 and BMNH2942A. The clavicles are also joined to each other and to the interclavicle in both specimens.



**Extended Data Figure 6 | Composite reconstruction of shoulder girdle and scapula-coracoid of eleutherodonts, in comparison to those of monotremes.** **a**, Reconstruction of shoulder girdle based on STL models of eleutherodont BMNH3258 (a juvenile, in ventral view); the interclavicle is not fully ossified and was reconstructed from the preserved interclavicles of BMNH2940, BMNH2942 and several other eleutherodonts with well preserved clavicle-interclavicles. **b**, Shoulder girdle of the monotreme *Tachyglossus* (adult). **c**, Shoulder girdle of the

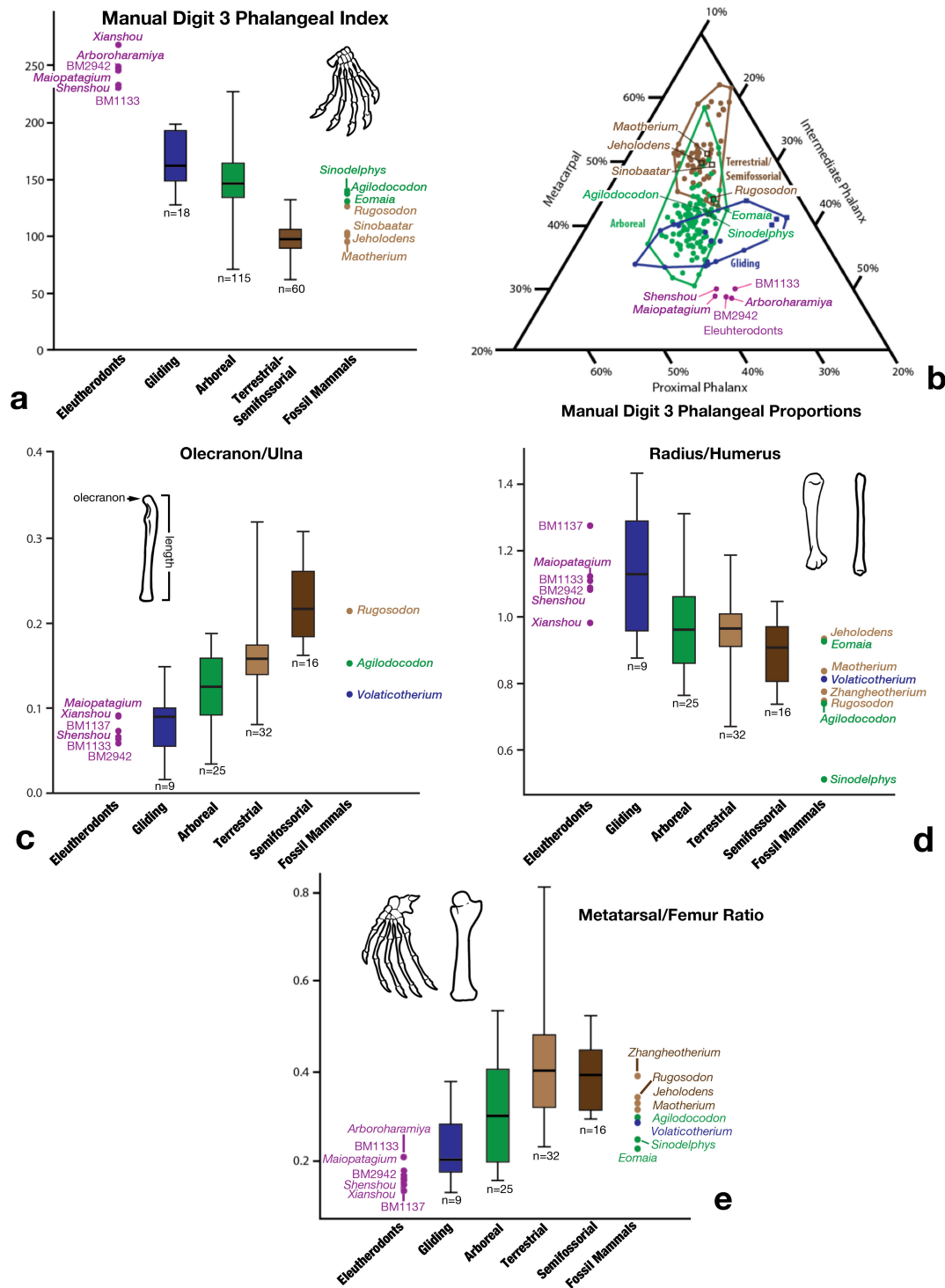
monotreme *Ornithorhynchus* (adult). **d**, Procoracoid, coracoid and scapula of a juvenile *Ornithorhynchus*. Note that the gracile coracoid, which is a juvenile feature, is similar to that of eleutherodonts. BMNH3258 is identified as a juvenile eleutherodont because it shows the lower permanent premolar in the process of erupting, and its shoulder girdle and partial forelimb elements are 80–85% the size of those on the adult specimen of *Maiopatagium*.





**Extended Data Figure 7 | Pedal structures of eleutherodonts with a bony (calcified) calcar.** **a**, An unnamed eleutherodont BMNH1133: right pes, showing that the calcar is distinct from, and coexists with, the os calcaris in this fossil. **b**, *Maiopatagium* (BMNH2940): right pes. Both specimens show a bony (calcified) calcar element that is articulated with the laterally bent calcaneal tuber by a contact of V-shaped trough and

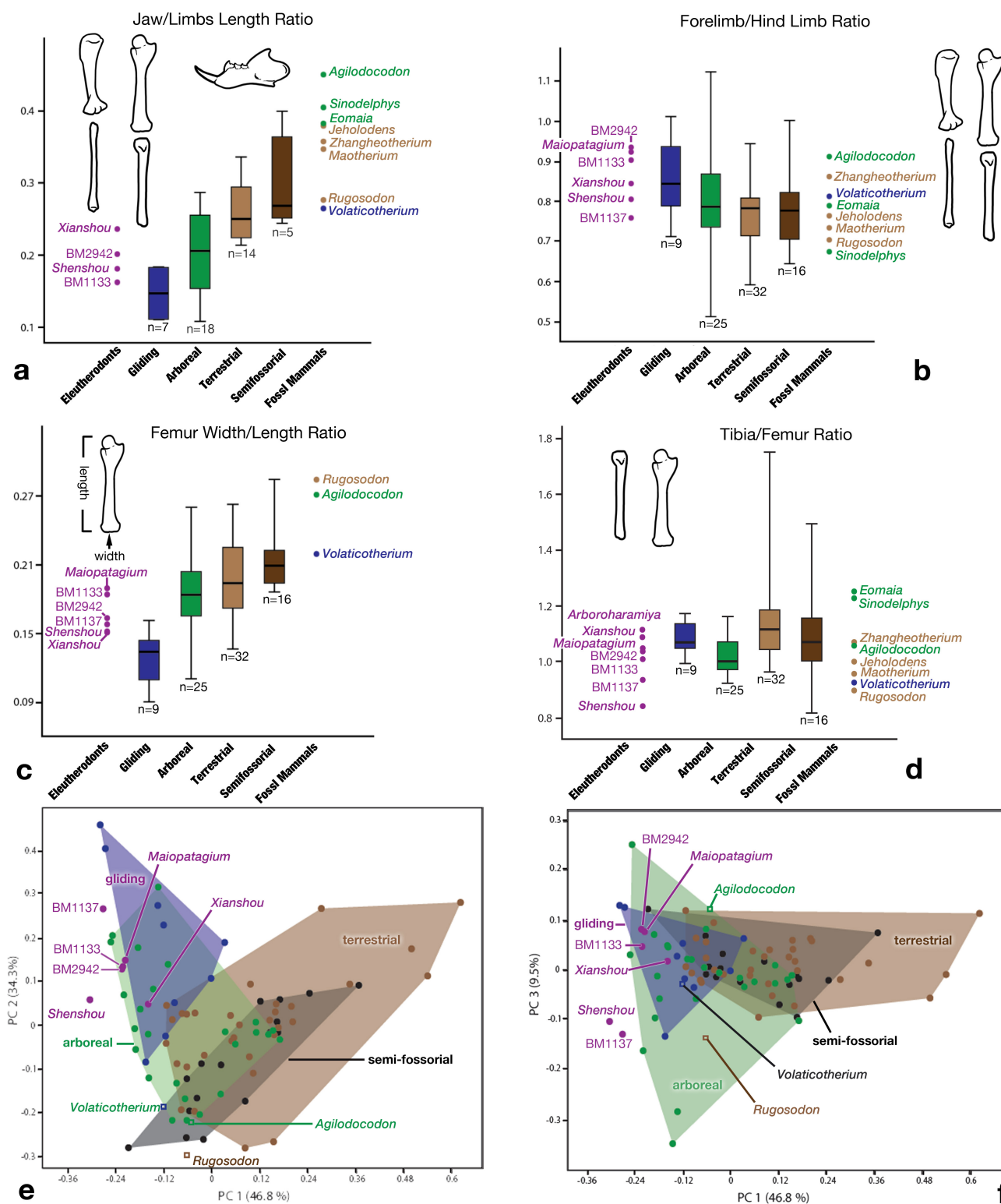
crest. This topographic relationship is identical to the calcar–calcaneus structural relationship of bats. Among a range of length and morphology of calcars in bats<sup>40</sup>, the eleutherodont calcar bears some resemblance to the short and stubby calcar of some bats (for example, *Desmodus*, among phyllostomid bats)<sup>41</sup>, although the base of the calcar is more conical and massive, distinctive from that of *Desmodus*<sup>41</sup>.



**Extended Data Figure 8 | Morphometric comparison of forelimb and manual structures of eleutherodonts and extant mammal ecomorphotypes.** **a**, Manual digit 3 phalangeal index. Eleutherodonts have more elongated manual phalanges than extant gliders and arborealists. **b**, Ternary distribution of intrinsic proportions of metacarpals, proximal phalanges, and intermediate phalanges of digit 3. Eleutherodont manual proportions are closest to those of extant mammals that are both arboreal and gliding, and are very similar to the pedal proportions of bats adapted to pedal roosting. **c**, Functional olecranon index, which is the ratio of olecranon length to length of the remainder of the ulna<sup>31,32</sup>. Eleutherodonts are well within the 25–75% quartiles of extant gliding mammals in having the shortest olecranon ratio, and they are below the lower 25% quartile of non-gliding arboreal mammals. The value range

of this index for eleutherodonts is consistent with the interpretation that they are mostly arboreal, and some are glissant. **d**, Brachial index, measured as the radius length divided by humerus length<sup>31</sup>. By this index, eleutherodonts are similar to extant mammalian gliders in having high brachial index ratios, although *Xianshou* and extant gliders partly overlap with the 25–75% quartiles of non-gliding arboreal mammals. **e**, Pedal length ratio (metatarsal length/femoral length) as an index for substrate preference. Eleutherodonts are most comparable to extant gliding mammals. The index supports previous inferences of *Agilodocodon*, *Eomaia* and *Sinodelphys* being scansorial/arboreal, although it is less supportive of the hypothesis that *Volaticotherium* is a glider (see Supplementary Table 9).





Extended Data Figure 9 | See next page for caption.

**Extended Data Figure 9 | Morphometrics of limb skeletons of eleutherodonts and extant mammals, and inference of preferred locomotor modes.** **a**, Ratio of dentary length to the summed lengths of forelimb and hindlimb as an index for substrate preference, as used by Meng *et al.*<sup>20</sup> to help infer that *Volaticotherium* is a glider. By this index, eleutherodonts are closest in values to extant gliders and arboreal mammals. However, we note that the eutriconodont *Volaticotherium*, the docodont *Agilodocodon*, and therians *Eomaia* and *Sinodelphys*, all of which had been inferred to be arboreal by qualitative morphological analyses, cannot be differentiated from extant terrestrial and semifossorial mammals by this index alone. Results suggest that *Volaticotherium* may not be a volant mammal, given our expanded reference dataset for this index. The efficacy of this index needs further study. **b**, Intermembral index is measured as the summed lengths of the humerus and radius divided by the summed lengths of the femur and tibia. Values for eleutherodonts overlap with both gliders and arborealists for this index.

**c**, Femoral epicondyle index, which is measured as the epicondylar width divided by the femoral length (as in ref. 31). **d**, Crural index, which is measured as the tibial length divided by femoral length. **e**, PCA of six functional indices (see Supplementary Information), showing the first two components (PC1 and PC2). Purple points are eleutherodonts, and squares are non-eleutherodont Mesozoic mammals. *Maiopatagium*, BMNH2942 and BMNH1133 are either nested in or close to the morphospace region (purple and blue polygon) of extant mammalian gliders, suggesting that they are gliders. *Volaticotherium* is separated from gliders along PC2, suggesting that it may not be a glider. **f**, PCA showing PC1 and PC3. *Maiopatagium*, BMNH2942, 1133, *Xianshou songae* and *Volaticotherium* occupy the same morphospace regions as modern gliders and arboreal taxa. However, *Shenshou* and BMNH1137 are separated from gliders, especially along PC3, and are closely associated with non-gliding arboreal mammals.



## Life Sciences Reporting Summary

Nature Research wishes to improve the reproducibility of the work that we publish. This form is intended for publication with all accepted life science papers and provides structure for consistency and transparency in reporting. Every life science submission will use this form; some list items might not apply to an individual manuscript, but all fields must be completed for clarity.

For further information on the points included in this form, see [Reporting Life Sciences Research](#). For further information on Nature Research policies, including our [data availability policy](#), see [Authors & Referees](#) and the [Editorial Policy Checklist](#).

### ► Experimental design

#### 1. Sample size

Describe how sample size was determined.

Our study reports on finding of original fossils. All fossil specimens available for this study has been have been reported. Their skeletal and dental measurements of the single holotype specimens and comparative measurements of skeletons of extant mammals are reported in supplementary information. Skeletal and dental measurement of the single holotype specimen and the body mass estimates of the new fossil species are reported in SI Tables S1, S2 and S3.

#### 2. Data exclusions

Describe any data exclusions.

No data on fossils available for this study have been excluded. All extant specimens for morphological comparison are also figured in the study. To the best of our ability, we exhausted sampling of all characters of the three main fossils used in this study. For ecomorphological morphometrical analyses, data from all extant comparative taxa that were measured are included in the quantitative analyses. Skeletal data from other early mammal taxa are compiled from existing literatures are all used in the analyses (SI Tables S3-S13)

#### 3. Replication

Describe whether the experimental findings were reliably reproduced.

For ecomorphological morphometrical analyses, data from all extant comparative taxa that were measured are included in the quantitative analyses. Skeletal data from other early mammal taxa are compiled from existing literatures are all used in the analyses (SI Tables S3-S13), to the best of our ability.

#### 4. Randomization

Describe how samples/organisms/participants were allocated into experimental groups.

Not applicable

#### 5. Blinding

Describe whether the investigators were blinded to group allocation during data collection and/or analysis.

Not applicable

Note: all studies involving animals and/or human research participants must disclose whether blinding and randomization were used.

## 6. Statistical parameters

For all figures and tables that use statistical methods, confirm that the following items are present in relevant figure legends (or in the Methods section if additional space is needed).

n/a Confirmed

- ☐ ☒ The exact sample size ( $n$ ) for each experimental group/condition, given as a discrete number and unit of measurement (animals, litters, cultures, etc.)
- ☒ ☐ A description of how samples were collected, noting whether measurements were taken from distinct samples or whether the same sample was measured repeatedly
- ☒ ☐ A statement indicating how many times each experiment was replicated
- ☒ ☐ The statistical test(s) used and whether they are one- or two-sided (note: only common tests should be described solely by name; more complex techniques should be described in the Methods section)
- ☒ ☐ A description of any assumptions or corrections, such as an adjustment for multiple comparisons
- ☒ ☐ The test results (e.g.  $P$  values) given as exact values whenever possible and with confidence intervals noted
- ☒ ☐ A clear description of statistics including central tendency (e.g. median, mean) and variation (e.g. standard deviation, interquartile range)
- ☒ ☐ Clearly defined error bars

See the web collection on [statistics for biologists](#) for further resources and guidance.

## ► Software

Policy information about [availability of computer code](#)

## 7. Software

Describe the software used to analyze the data in this study.

Not applicable

For manuscripts utilizing custom algorithms or software that are central to the paper but not yet described in the published literature, software must be made available to editors and reviewers upon request. We strongly encourage code deposition in a community repository (e.g. GitHub). *Nature Methods* [guidance for providing algorithms and software for publication](#) provides further information on this topic.

## ► Materials and reagents

Policy information about [availability of materials](#)

## 8. Materials availability

Indicate whether there are restrictions on availability of unique materials or if these materials are only available for distribution by a for-profit company.

The morphometrical data are already included in the online Supplementary Information at Nature.Com. The STL files on the shoulder Girdle of BMNH3258 from the CT scanning will be deposited in MorphoSource.Org, a public repository of CT-derived data. Because we are still working on a separate functional analysis with the shoulder girdle and forelimb from the master CT dataset, we cannot yet release the raw CT dataset that is under active study for other structures, which cannot be covered by short Nature paper.

## 9. Antibodies

Describe the antibodies used and how they were validated for use in the system under study (i.e. assay and species).

Not applicable

## 10. Eukaryotic cell lines

a. State the source of each eukaryotic cell line used.

Not applicable

b. Describe the method of cell line authentication used.

Not applicable

c. Report whether the cell lines were tested for mycoplasma contamination.

Not applicable

d. If any of the cell lines used are listed in the database of commonly misidentified cell lines maintained by [ICLAC](#), provide a scientific rationale for their use.

Not applicable



► Animals and human research participants

Policy information about [studies involving animals](#); when reporting animal research, follow the [ARRIVE guidelines](#)

11. Description of research animals

Provide details on animals and/or animal-derived materials used in the study.

Not applicable

Policy information about [studies involving human research participants](#)

12. Description of human research participants

Describe the covariate-relevant population characteristics of the human research participants.

Not applicable